Resonant Dipole-Dipole Interaction and 3D Complete Optical Shielding

Xiao Chai*

Department of Physics, Fudan University,

Shanghai 200433, People's Republic of China

(Dated: May 23, 2017)

Abstract

We summarize a semi-classical method to simulate the dynamics of two atoms in near resonant light fields. Both internal state dynamics and external motion are considered. The full hyperfine structure of alkali atoms is included. We apply this method to study the possibility of 3D complete optical shielding in cold atom system with proper engineered laser fields.

Instructor: Prof. Saijun Wu

I. INTRODUCTION

Study of quantum degeneracy in cold atomic system requires extremely high atomic density. When the density reaches about 10^{12} cm^{-3} [1], atom-atom interaction will play an important role in laser cooling and trapping. In short range, hyperfine-changing collision, radiative escape, and fine-structure-changing collisions are the main processes that lead to trap loss [2]. Such collisional trap loss and heating constrain the density and temperature that can be reached through purely optical method.

On the other hand, research of many-body physics in ultracold quantum gas requires advanced imaging techniques. A basic example is imaging of multiple atoms in experimental realization of Bose-Hubbard model. Non-destructive detection of multiple atoms in single lattice site is, however, limited by resonant interaction between atoms [3].

Optical suppression of inelastic collisions is a potential solution to the above two problems. Such method is called optical shielding, which is studied intensively in the last century [4–7]. The basic idea of this method is to shine blue detuned laser beams upon atomic gas. As two atoms approaching each other, the blue detuned beams will couple the two-atom ground state $S + S$ with the molecular state $S + P$ around Condon point R_C. Consequently the dressed ground state will feel an effective repulsive potential and the two atoms will recede from each other elastically, as shown in Fig. 6. If R_C is properly chosen by setting a proper detuning, those short range (≤ 10 nm[2]) inelastic processes can be avoided. In this way the trap loss can be suppressed and non-destructive observation of multiple atoms in single site is made possible.

However, the research of optical shielding stagnate since last century. The 3D nature of collision, the complex hyperfine structure of atoms, quantum jump and recoil are hard parts of this problem, which are partly ignored by some early work. Some papers present analytical calculation of shielding measure using simple Landau-Zener theory [4, 6]. Nevertheless, the stochastic nature of atomic motion in laser field indicates that a statistical way of study is more convincing. Thus, in this paper we present a theoretical framework of long range dipole-dipole interaction including all the effects mentioned above. Based on the theory, we give some semi-classical MCWF (Monte Carlo wave-function method) simulation results and compare them with experimental results. In principal we can do full quantum simulation to include the wave nature of atomic motion, as done by Suominen [8]. However, a full

quantum 3D simulation is not applicable since it consumes too much computational resource. In addition, simulation with quantized internal states and classical atomic motion has been proved work well for sub-Doppler D1 cooling [9]. For these reasons, we adopt a semi-classical way of study here.

The paper is organized as follows. In Sec. II, the master equation governing two atoms with hyperfine structure is derived and it is unrevealed to quantum trajectory theory in preparation for simulation. In Sec. III, the simulation method and results are given. In Sec. IV we compare the simulation with a simple qualitative experiment.

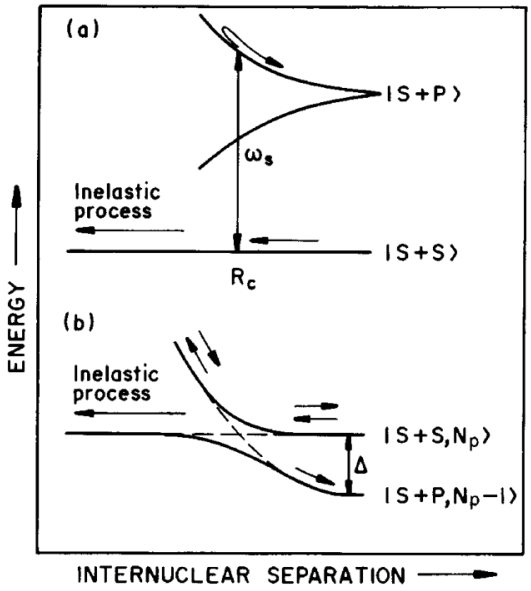

FIG. 1: This Fig. is from Bagnato 1997 [7]. (a) Atoms approach with each other in the ground state and excited around Condon point R_C to the repulsive excited state. (b) Dressed state picture.

II. THEORY

II.1. Two Atom Master Equation

The standard way to study the dynamics of atoms interfered by vacuum electromagnetic field is master equation method. Following the procedure of Born-Markov approximation and elimination of the vacuum modes, we can formulate the master equation governing the

internal dynamics of two atoms. Interestingly, resonant dipole-dipole interaction terms will also arise in this procedure. In another word, atoms interact with each other via vacuum modes. Here we give a detailed deduction of the master equation based on the work of Meystre [10, 11].

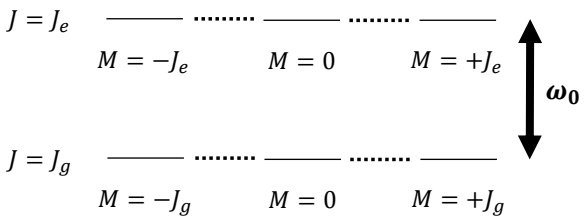

FIG. 2: A $J = J_g \to J = J_e$ system. The ground state and excited state have angular quantum number J_g and J_e respectively. The atomic transition frequency is ω_0.

We consider a system composed of two identical atoms and the quantized vacuum electromagnetic field. We assume the two atoms are fixed at position $\boldsymbol{r}_1, \boldsymbol{r}_2$ and ignore the external dynamics for now. The mechanical effects of vacuum perturbation will be discussed in Sec. II.4. For simplicity, we model the internal state of atom as a $J = J_g \to J = J_e$ system as shown in Fig. 2. Thus, the basis of the Hilbert space is

$$|J_1, M_1\rangle_1 \otimes |J_2, M_2\rangle_2 \otimes |n\rangle_{\boldsymbol{k},\sigma}\,, \tag{1}$$

where J_i denotes ground or excited state, i.e. $J_i = J_g$ or J_e; $M_i = -J_i, -J_i+1, \cdots J_i-1, J_i$; $|n\rangle_{\boldsymbol{k},\sigma}$ is the fock state of the mode with wave vector $\boldsymbol{k}$ and polarization σ.

The Hamiltonian of the system is composed of three terms

$$H = H_a + H_f + H_{af}. \tag{2}$$

The first term

$$H_a = \hbar\omega_0 \sum_{i=1}^{2} P_e^i \tag{3}$$

is the unperturbed Hamiltonian of the two atoms. Here ω_0 is the atomic transition frequency. P_e^i is the projection operator of excited state of the ith atom,

$$P_e^i = \sum_{M=-J_e}^{+J_e} |J_e, M\rangle_{i\,i}\langle J_e, M|. \tag{4}$$

Actually P_e^i is a tensor product of the projection operator acting on the Hilbert space of the ith atom and the identical operator acting on the Hilbert composed of the other atom and the field. For simplicity we omit the tensor product procedure.

The second term is the free space Hamiltonian,

$$H_f = \sum_{\boldsymbol{k},\sigma} \hbar\omega_k a^\dagger_{\boldsymbol{k},\sigma} a_{\boldsymbol{k},\sigma}, \tag{5}$$

where $a^\dagger_{\boldsymbol{k},\sigma}$ and $a_{\boldsymbol{k},\sigma}$ are creation and annihilation operator of the $\boldsymbol{k},\sigma$ mode. $\omega_k = kc$ is the frequency of the mode.

The third term corresponds to atom-field coupling. Under dipole approximation,

$$H_{af} = -\sum_{i=1}^{2} \boldsymbol{E}(\boldsymbol{r}_i)\cdot\boldsymbol{d}^i, \tag{6}$$

where $\boldsymbol{d}^i$ is the dipole operator of the ith atom. $\boldsymbol{E}(\boldsymbol{r}_i)$ is the field operator at $\boldsymbol{r}_i$,

$$\boldsymbol{E}(\boldsymbol{r}) = \sum_{\boldsymbol{k},\sigma} \hat{\boldsymbol{\epsilon}}_{\boldsymbol{k},\sigma}\mathscr{E}_k a^\dagger_{\boldsymbol{k},\sigma} \mathrm{e}^{-\mathrm{i}\boldsymbol{k}\cdot\boldsymbol{r}} + \mathrm{H.c.}. \tag{7}$$

$\hat{\boldsymbol{\epsilon}}_{\boldsymbol{k},\sigma}$ is a set of unit polarization vectors perpendicular to $\boldsymbol{k}$ with $\sigma = \pm 1$. $\mathscr{E}_k$ is the single photon electric field intensity,

$$\mathscr{E}_k = \sqrt{\frac{\hbar\omega_k}{2\epsilon_0 V}}, \tag{8}$$

where ϵ_0 is the vacuum permittivity, V is the quantization volume. The choosing of $\hat{\boldsymbol{\epsilon}}_{\boldsymbol{k},\sigma}$ is arbitrary as long as the two polarization vectors are linear independent and perpendicular to $\boldsymbol{k}$. The set of helicity polarization vectors is a convenient choice:

$$\hat{\boldsymbol{\epsilon}}_{\boldsymbol{k},\sigma} = R(\hat{\boldsymbol{k}})\hat{\boldsymbol{e}}_\sigma. \tag{9}$$

Here $R(\hat{\boldsymbol{k}})$ is the rotation matrix transforming unit vector in z-direction to $\hat{\boldsymbol{k}}$: $R(\hat{\boldsymbol{k}})\hat{\boldsymbol{z}} = \hat{\boldsymbol{k}}$. $\hat{\boldsymbol{e}}_\sigma$ are spherical bases with $\sigma = \pm 1$:

$$\hat{\boldsymbol{e}}_{+1} = -\frac{\hat{\boldsymbol{x}} + \mathrm{i}\hat{\boldsymbol{y}}}{\sqrt{2}} \tag{10}$$

$$\hat{\boldsymbol{e}}_0 = \hat{\boldsymbol{z}} \tag{11}$$

$$\hat{\boldsymbol{e}}_{-1} = \frac{\hat{\boldsymbol{x}} - \mathrm{i}\hat{\boldsymbol{y}}}{\sqrt{2}}. \tag{12}$$

We can expand dipole operator $\boldsymbol{d}$ in the atomic basis $|J, M\rangle$:

$$\boldsymbol{d} = \sum_{M,M'} \langle J_g, M|\,\boldsymbol{d}\,|J_e, M'\rangle\,|J_g, M\rangle\,\langle J_e, M'| + \mathrm{H.c.}. \tag{13}$$

Here we omit the diagonal terms because these terms are equal to zero due to parity. Accordingly, under rotating wave approximation Eq. (6) becomes

$$H_{af} = -\sum_{i,\boldsymbol{k},\sigma,M,M'} \mathscr{E}_k a^\dagger_{\boldsymbol{k},\sigma} \mathrm{e}^{-\mathrm{i}\boldsymbol{k}\cdot\boldsymbol{r}_i} \langle J_g, M| \hat{\boldsymbol{\epsilon}}_{\boldsymbol{k},\sigma}\cdot\boldsymbol{d} |J_e, M'\rangle |J_g, M\rangle_{i\,i}\langle J_e, M'| + \mathrm{H.c.}. \tag{14}$$

Expanding $\boldsymbol{d}$ in spherical basis, we have

$$\boldsymbol{d} = \sum_q d_q \hat{\boldsymbol{e}}^*_q, \tag{15}$$

where $q = 0, \pm 1$ and $d_q = \boldsymbol{d}\cdot\hat{\boldsymbol{e}}_q$. According to Eq. (9) and Eq. (15), we rewrite $\hat{\boldsymbol{\epsilon}}_{\boldsymbol{k},\sigma}\cdot\boldsymbol{d}$ in Eq. (14) as

$$\begin{aligned}
\hat{\boldsymbol{\epsilon}}_{\boldsymbol{k},\sigma}\cdot\boldsymbol{d} &= \sum_q (R(\hat{\boldsymbol{k}})\hat{\boldsymbol{e}}_\sigma)\cdot(d_q\hat{\boldsymbol{e}}^*_q) = \sum_{q,q'} (D^1_{q',\sigma}(\hat{\boldsymbol{k}})\hat{\boldsymbol{e}}_{q'})\cdot(d_q\hat{\boldsymbol{e}}^*_q) \\
&= \sum_{q,q'} D^1_{q,\sigma}(\hat{\boldsymbol{k}}) d_q (\hat{\boldsymbol{e}}^*_q\cdot\hat{\boldsymbol{e}}_{q'}) \\
&= \sum_q D^1_{q,\sigma}(\hat{\boldsymbol{k}}) d_q.
\end{aligned} \tag{16}$$

Here we have applied the orthogonality and rotation property of spherical basis. $D^1_{q,\sigma}(\hat{\boldsymbol{k}})$ is the Wigner D-matrix corresponding to the rotation $R(\hat{\boldsymbol{k}})$.

According to Wigner-Eckart theorem,

$$\langle J_g, M|\, d_q\, |J_e, M'\rangle = \langle J_g\|d\|J_e\rangle\langle J_g, M|J_e, 1, M', q\rangle. \tag{17}$$

Here $\langle J_g, M|J_e, 1, M', q\rangle$ is the Clebsch-Gordan coefficient with $q = 0, \pm 1$. Based on the selection rules of the Clebsch-Gordan coefficient, we have $M' = M - q$. $\langle J_g\|d\|J_e\rangle$ is the reduced matrix element, which is a fixed c-number depends on J_g, J_e and $\boldsymbol{d}$. We denote $\langle J_g\|d\|J_e\rangle$ as $\mathfrak{p}$. According to Eq. (16) and Eq. (17), we rewrite Eq. (14) as

$$H_{af} = -\sum_{i,\boldsymbol{k},\sigma,M,q} \mathfrak{p}\mathscr{E}_k D^1_{q,\sigma}(\hat{\boldsymbol{k}}) \mathrm{e}^{-\mathrm{i}\boldsymbol{k}\cdot\boldsymbol{r}_i} a^\dagger_{\boldsymbol{k},\sigma} \langle J_g, M|J_e, 1, M-q, q\rangle |J_g, M\rangle_{i\,i}\langle J_e, M-q| + \mathrm{H.c.}. \tag{18}$$

Define the jump operator S^i_q as

$$S^i_q = \sum_M \langle J_g, M|J_e, 1, M-q, q\rangle |J_g, M\rangle_{i\,i}\langle J_e, M|. \tag{19}$$

Thus, Eq. (18) becomes

$$H_{af} = -\sum_{i,\boldsymbol{k},\sigma,q} \mathfrak{p}\mathscr{E}_k D^1_{q,\sigma}(\hat{\boldsymbol{k}}) \mathrm{e}^{-\mathrm{i}\boldsymbol{k}\cdot\boldsymbol{r}_i} a^\dagger_{\boldsymbol{k},\sigma} S^i_q + \mathrm{H.c.}. \tag{20}$$

In interaction picture, Eq. (20) transforms to

$$\tilde{H}_{af} = -\sum_{i,\boldsymbol{k},\sigma,q} \mathfrak{p}\mathscr{E}_k D^1_{q,\sigma}(\hat{\boldsymbol{k}}) \mathrm{e}^{-\mathrm{i}\boldsymbol{k}\cdot\boldsymbol{r}_i - \mathrm{i}(\omega_0-\omega_k)t} a^\dagger_{\boldsymbol{k},\sigma} S^i_q + \mathrm{H.c.}. \tag{21}$$

For clarity, we give the range of value for the indexes in Eq. (21) below:

$$\begin{cases} i & : \ 1,2 \\ \boldsymbol{k} & : \ \text{full } \boldsymbol{k}\text{-space} \\ \sigma & : \ \pm 1 \\ q & : \ 0, \pm 1. \end{cases} \tag{22}$$

The dynamics of the system's density matrix ρ_{af} is given by the Liouville - von Neumann equation:

$$\dot{\rho}_{af}(t) = -\frac{\mathrm{i}}{\hbar}[\tilde{H}_{af}(t), \rho_{af}(t)]. \tag{23}$$

Following the standard procedure of Born-Markov approximation, we have the equation of the atomic density matrix:

$$\dot{\rho}_a(t) = -\frac{1}{\hbar^2}\mathrm{tr}_f \int_0^t \mathrm{d}\tau \ [\tilde{H}_{af}(t), [\tilde{H}_{af}(\tau), \rho_a(t) \otimes \rho_f(0)]]. \tag{24}$$

Here we have assumed $\rho_{af}(\tau)$ can be decomposed into the direct product of $\rho_a(\tau)$ and $\rho_f(\tau)$. The field is assumed to be in equilibrium, i.e. $\rho_f(\tau) \approx \rho_f(0)$. The atomic system is assumed to have no memory, i.e. $\rho_a(\tau) \approx \rho_a(t)$. tr_f represents tracing off the field degree of freedom. We assume the field is a reservoir at zero temperature. It can be shown that

$$\mathrm{tr}_f(\rho_f a_{\boldsymbol{k},\sigma}) = \mathrm{tr}_f(\rho_f a^\dagger_{\boldsymbol{k},\sigma}) = 0 \tag{25}$$

$$\mathrm{tr}_f(\rho_f a_{\boldsymbol{k},\sigma} a_{\boldsymbol{k}',\sigma'}) = \mathrm{tr}_f(\rho_f a^\dagger_{\boldsymbol{k},\sigma} a^\dagger_{\boldsymbol{k}',\sigma'}) = 0 \tag{26}$$

$$\mathrm{tr}_f(\rho_f a^\dagger_{\boldsymbol{k},\sigma} a_{\boldsymbol{k}',\sigma'}) = 0 \tag{27}$$

$$\mathrm{tr}_f(\rho_f a_{\boldsymbol{k},\sigma} a^\dagger_{\boldsymbol{k}',\sigma'}) = \delta_{\boldsymbol{k},\boldsymbol{k}'}\delta_{\sigma,\sigma'}, \tag{28}$$

Where $\delta_{\boldsymbol{k},\boldsymbol{k}'}$ and $\delta_{\sigma,\sigma'}$ are Kroneker delta symbols. Thus, Eq. (24) gives

$$\begin{aligned} \dot{\rho}_a(t) = -\frac{|\mathfrak{p}|^2}{\hbar^2}\int_0^t \mathrm{d}\tau \sum_{\boldsymbol{k},\sigma,i,i',q,q'} \mathscr{E}^2_k (& \mathrm{e}^{\mathrm{i}(\omega_0-\omega_k)(t-\tau)} \mathrm{e}^{\mathrm{i}\boldsymbol{k}\cdot(\boldsymbol{r}_i-\boldsymbol{r}_{i'})} D^{1*}_{q,\sigma}(\hat{\boldsymbol{k}}) D^1_{q',\sigma}(\hat{\boldsymbol{k}}) S^{i\dagger}_q S^{i'}_{q'} \rho_a(t) \\ & - \mathrm{e}^{\mathrm{i}(\omega_0-\omega_k)(t-\tau)} \mathrm{e}^{\mathrm{i}\boldsymbol{k}\cdot(\boldsymbol{r}_i-\boldsymbol{r}_{i'})} D^{1*}_{q,\sigma}(\hat{\boldsymbol{k}}) D^1_{q',\sigma}(\hat{\boldsymbol{k}}) S^{i'}_{q'} \rho_a(t) S^{i\dagger}_q \\ & - \mathrm{e}^{-\mathrm{i}(\omega_0-\omega_k)(t-\tau)} \mathrm{e}^{\mathrm{i}\boldsymbol{k}\cdot(\boldsymbol{r}_i-\boldsymbol{r}_{i'})} D^{1*}_{q,\sigma}(\hat{\boldsymbol{k}}) D^1_{q',\sigma}(\hat{\boldsymbol{k}}) S^{i'}_{q'} \rho_a(t) S^{i\dagger}_q \\ & + \mathrm{e}^{-\mathrm{i}(\omega_0-\omega_k)(t-\tau)} \mathrm{e}^{\mathrm{i}\boldsymbol{k}\cdot(\boldsymbol{r}_i-\boldsymbol{r}_{i'})} D^{1*}_{q,\sigma}(\hat{\boldsymbol{k}}) D^1_{q',\sigma}(\hat{\boldsymbol{k}}) \rho_a(t) S^{i\dagger}_q S^{i'}_{q'}). \end{aligned} \tag{29}$$

To calculate the integral, it is convenient to introduce relative coordinates $\boldsymbol{r}, \boldsymbol{R}$ and formal jump operators $A_{1,q}, A_{2,q}$. Define

$$\boldsymbol{R} = \frac{\boldsymbol{r}_2 + \boldsymbol{r}_1}{2} \tag{30}$$

$$\boldsymbol{r} = \boldsymbol{r}_2 - \boldsymbol{r}_1 \tag{31}$$

$$A_{1,q} = S_q^1 - S_q^2 \tag{32}$$

$$A_{2,q} = S_q^1 + S_q^2. \tag{33}$$

We rewrite equation Eq. (29) in terms of the above symbols:

$$\begin{aligned}\dot{\rho}_a(t) = -\frac{|\mathfrak{p}|^2}{\hbar^2}\int_0^t \mathrm{d}\tau \sum_{\boldsymbol{k},\sigma,q,q'} \mathscr{E}_k^2 \\ (\mathrm{e}^{\mathrm{i}(\omega_0-\omega_k)(t-\tau)}(X^*_{1,q,\sigma,\boldsymbol{k}}A^\dagger_{1,q} + X^*_{2,q,\sigma,\boldsymbol{k}}A^\dagger_{2,q})(X_{1,q',\sigma,\boldsymbol{k}}A_{1,q'} + X_{2,q',\sigma,\boldsymbol{k}}A_{2,q'})\rho_a(t) \\ -\mathrm{e}^{\mathrm{i}(\omega_0-\omega_k)(t-\tau)}(X_{1,q',\sigma,\boldsymbol{k}}A_{1,q'} + X_{2,q',\sigma,\boldsymbol{k}}A_{2,q'})\rho_a(t)(X^*_{1,q,\sigma,\boldsymbol{k}}A^\dagger_{1,q} + X^*_{2,q,\sigma,\boldsymbol{k}}A^\dagger_{2,q}) \\ -\mathrm{e}^{-\mathrm{i}(\omega_0-\omega_k)(t-\tau)}(X_{1,q',\sigma,\boldsymbol{k}}A_{1,q'} + X_{2,q',\sigma,\boldsymbol{k}}A_{2,q'})\rho_a(t)(X^*_{1,q,\sigma,\boldsymbol{k}}A^\dagger_{1,q} + X^*_{2,q,\sigma,\boldsymbol{k}}A^\dagger_{2,q}) \\ +\mathrm{e}^{-\mathrm{i}(\omega_0-\omega_k)(t-\tau)}\rho_a(t)(X^*_{1,q,\sigma,\boldsymbol{k}}A^\dagger_{1,q} + X^*_{2,q,\sigma,\boldsymbol{k}}A^\dagger_{2,q})(X_{1,q',\sigma,\boldsymbol{k}}A_{1,q'} + X_{2,q',\sigma,\boldsymbol{k}}A_{2,q'})),\end{aligned} \tag{34}$$

where

$$X_{1,q,\sigma,\boldsymbol{k}} = -D^1_{q,\sigma}(\hat{\boldsymbol{k}})\cos(\boldsymbol{k}\cdot\boldsymbol{r}/2) \tag{35}$$

$$X_{2,q,\sigma,\boldsymbol{k}} = -\mathrm{i}D^1_{q,\sigma}(\hat{\boldsymbol{k}})\sin(\boldsymbol{k}\cdot\boldsymbol{r}/2). \tag{36}$$

Through the standard prescription, the sum over $\boldsymbol{k}$ can be replaced by

$$\sum_{\boldsymbol{k}} \to \frac{V}{(2\pi)^3}\int_0^\infty \mathrm{d}k\ k^2 \int \mathrm{d}\Omega_k. \tag{37}$$

Now we focus on the first term of Eq. (34), i.e.

$$\begin{aligned}-\frac{|\mathfrak{p}|^2 V}{(2\pi)^3\hbar^2}\sum_{q,q'}\int_0^\infty \mathrm{d}k\ k^2\mathscr{E}_k^2\int_0^t \mathrm{d}\tau\ \mathrm{e}^{\mathrm{i}(\omega_0-\omega_k)(t-\tau)}(I^{11}_{q,q'}(k)A^\dagger_{1,q}A_{1,q'} + I^{12}_{q,q'}(k)A^\dagger_{1,q}A_{2,q'} \\ +I^{21}_{q,q'}(k)A^\dagger_{2,q}A_{1,q'} + I^{22}_{q,q'}(k)A^\dagger_{2,q}A_{2,q'})\rho_a(t),\end{aligned} \tag{38}$$

where

$$I^{ij}_{q,q'}(k) = \sum_\sigma \int \mathrm{d}\Omega_k\ X^*_{i,q,\sigma,\boldsymbol{k}}X_{j,q',\sigma,\boldsymbol{k}}. \tag{39}$$

The time integral in Eq. (38) is standard. We give the result under Markov approximation here:

$$\int_0^t \mathrm{d}\tau\ \mathrm{e}^{\mathrm{i}(\omega_0-\omega_k)(t-\tau)} \approx \int_0^\infty \mathrm{d}\tau\ \mathrm{e}^{\mathrm{i}(\omega_0-\omega_k)\tau} = \pi\delta(\omega_0-\omega_k) + \mathrm{i}P(\frac{1}{\omega_0-\omega_k}), \tag{40}$$

where $P(1/(\omega_0-\omega_k))$ denotes Cauchy principle value and $\delta(\omega_0-\omega_k)$ is the Dirac delta function. The calculation of $I^{ij}_{q,q'}(k)$ is tedious but straight forward. We give a detailed deduction in App. A. The result is listed below:

$$I^{11}_{q,q'}(k)=\frac{\pi}{3}(\beta_{q,q'}(k,\boldsymbol{r})+4\delta_{q,q'}) \tag{41}$$

$$I^{22}_{q,q'}(k)=\frac{\pi}{3}(-\beta_{q,q'}(k,\boldsymbol{r})+4\delta_{q,q'}) \tag{42}$$

$$I^{12}_{q,q'}(k)=I^{21}_{q,q'}(k)=0, \tag{43}$$

where $\beta(k,\boldsymbol{r})$ is a 3×3 Hermitian matrix with index runs from -1 to $+1$:

$$\begin{pmatrix} 4j_0(kr)-2j_2(kr)P_2(\cos\theta_r) & -\sqrt{2}\mathrm{e}^{-\mathrm{i}\phi_r}j_2(kr)P_2^1(\cos\theta_r) & -\mathrm{e}^{-2\mathrm{i}\phi_r}j_2(kr)P_2^2(\cos\theta_r) \\ -\sqrt{2}\mathrm{e}^{-\mathrm{i}\phi_r}j_2(kr)P_2^1(\cos\theta_r) & 4j_0(kr)+4j_2(kr)P_2(\cos\theta_r) & \sqrt{2}\mathrm{e}^{-\mathrm{i}\phi_r}j_2(kr)P_2^1(\cos\theta_r) \\ -\mathrm{e}^{-2\mathrm{i}\phi_r}j_2(kr)P_2^2(\cos\theta_r) & \sqrt{2}\mathrm{e}^{-\mathrm{i}\phi_r}j_2(kr)P_2^1(\cos\theta_r) & 4j_0(kr)-2j_2(kr)P_2(\cos\theta_r) \end{pmatrix}. \tag{44}$$

Here r,θ_r,ϕ_r are spherical coordinates of the relative position $\boldsymbol{r}$; $j_i(kr)$ denotes spherical Bessel function of the first kind with order i; $P_i^j(\cos\theta_r)$ denotes associated Legendre function with order i,j. The remaining k-integral in Eq. (38) gives the final damping terms and dipole-dipole interaction terms. Specifically, the first term of Eq. (40) gives rise to damping and the second term of Eq. (40) gives rise to dipole-dipole interaction. The integral with the kernel $\delta(\omega_0-\omega_k)$ is trivial, while the integral with the kernal $P(1/(\omega_0-\omega_k))$ requires some work. We give the deduction in App. B and the final form of Eq. (38) below:

$$-\frac{\Gamma}{16}\sum_{q,q'}[(\beta_{q,q'}(k_0,\boldsymbol{r})+4\delta_{q,q'}+\mathrm{i}\alpha_{q,q'}(k_0,\boldsymbol{r}))A^\dagger_{1,q}A_{1,q'}+(-\beta_{q,q'}(k_0,\boldsymbol{r})+4\delta_{q,q'}-\mathrm{i}\alpha_{q,q'}(k_0,\boldsymbol{r}))A^\dagger_{1,q}A_{1,q'}]\rho_a(t), \tag{45}$$

where

$$\Gamma=\frac{\omega_0^3|\mathfrak{p}|^2}{3\pi\epsilon_0\hbar c^3} \tag{46}$$

is the natural line width; $k_0=\omega_0/c$ is the magnitude of the wave vector corresponding to the resonant frequency; $\alpha(k,\boldsymbol{r})$ is another 3×3 Hermitian matrix:

$$\begin{pmatrix} 4n_0(kr)-2n_2(kr)P_2(\cos\theta_r) & -\sqrt{2}\mathrm{e}^{-\mathrm{i}\phi_r}n_2(kr)P_2^1(\cos\theta_r) & -\mathrm{e}^{-2\mathrm{i}\phi_r}n_2(kr)P_2^2(\cos\theta_r) \\ -\sqrt{2}\mathrm{e}^{-\mathrm{i}\phi_r}n_2(kr)P_2^1(\cos\theta_r) & 4n_0(kr)+4n_2(kr)P_2(\cos\theta_r) & \sqrt{2}\mathrm{e}^{-\mathrm{i}\phi_r}n_2(kr)P_2^1(\cos\theta_r) \\ -\mathrm{e}^{-2\mathrm{i}\phi_r}n_2(kr)P_2^2(\cos\theta_r) & \sqrt{2}\mathrm{e}^{-\mathrm{i}\phi_r}n_2(kr)P_2^1(\cos\theta_r) & 4n_0(kr)-2n_2(kr)P_2(\cos\theta_r) \end{pmatrix}. \tag{47}$$

Here $n_i(kr)$ denotes spherical Bessel function of the second kind with order i.

The deduction for the rest of terms in Eq. (34) is similar. We give the final form of the master equation here:

$$\begin{aligned}\dot{\rho}_a(t) =&\frac{1}{16}\Gamma\sum_{q,q'}(-i[\alpha_{q,q'}(k_0,\boldsymbol{r})(A^\dagger_{1,q}A_{1,q'}-A^\dagger_{2,q}A_{2,q'}),\rho_a(t)]\\&-(\beta_{q,q'}(k_0,\boldsymbol{r})+4\delta_{qq'})(A^\dagger_{1,q}A_{1,q'}\rho_a(t)+\rho_a(t)A^\dagger_{1,q}A_{1,q'}-2A_{1,q'}\rho_a(t)A^\dagger_{1,q})\\&-(-\beta_{q,q'}(k_0,\boldsymbol{r})+4\delta_{qq'})(A^\dagger_{2,q}A_{2,q'}\rho_a(t)+\rho_a(t)A^\dagger_{2,q}A_{2,q'}-2A_{2,q'}\rho_a(t)A^\dagger_{2,q}))\end{aligned} \tag{48}$$

II.2. Hyperfine Structure

In a realistic problem, we have to deal with near-degenerate energy levels induced by hyperfine interaction. We will take the D1 structure of ^{39}K as an example in our simulation. As shown in Fig. 3, the ^{39}K D1 structure has two sets of ground states and two sets of

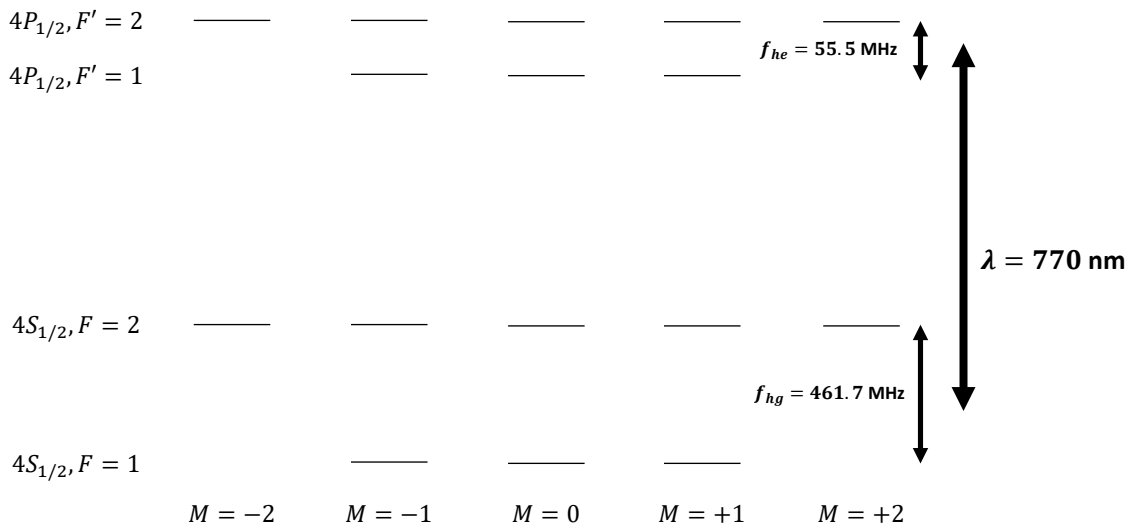

FIG. 3: ^{39}K D1 structure.

excited states. The deduction of the master equation in such a near-degenerate system is slightly different from Sec. II.1. Typically, the terms $e^{i(\omega_1-\omega_k)t-i(\omega_2-\omega_k)\tau}$ will arise in the time integral (40), with $\omega_1 \approx \omega_2$, thus it will be hard to calculate the integral. We give a brief solution to this problem here.

The eigenstates of single atom are now composed by $|F, M\rangle$. As shown in Fig. 3, we denote excited states with F' and ground states with F. For D1, $F = 1$ or 2 and $F' = 1$ or 2. In addition, we denote the atomic frequencies with $\omega_{FF'}$. For example, ω_{12} is the atomic

transition frequency of $F=1\to F'=2$. Since $\omega_{FF'}\gg\omega_{hg},\omega_{he}$, we have $\omega_{11}\approx\omega_{12}\approx\omega_{21}\approx\omega_{22}\approx\omega_0$ (ω_{hg},ω_{he} are hyperfine splitting of the ground and excited states). Now the atomic Hamiltonian in Eq. (3) turns to

$$H_a=\hbar\sum_i(\omega_{1F'}\sum_{F',M}|F',M\rangle_{i\,i}\langle F',M|+\omega_{hg}\sum_M|F=2,M\rangle_{i\,i}\langle F=2,M|), \tag{49}$$

where we have assumed the state $|F=1,M\rangle$ is the zero energy point. And the atom-field couping Hamiltonian (21) in interaction picture turns to

$$\tilde{H}_{af}=-\sum_{i,\boldsymbol{k},\sigma,q,F,F'}\mathfrak{p}\mathscr{E}_k D^1_{q,\sigma}(\hat{\boldsymbol{k}})\mathrm{e}^{-\mathrm{i}\boldsymbol{k}\cdot\boldsymbol{r}_i-\mathrm{i}(\omega_{FF'}-\omega_k)t}a^\dagger_{\boldsymbol{k},\sigma}S^i_{F,F',q}+\mathrm{H.c.}, \tag{50}$$

where

$$S^i_{F,F',q}=\sum_M\langle F,M|F',1,M-q,q\rangle\,|F,M\rangle_{i\,i}\langle F',M|. \tag{51}$$

Then Eq. (29) becomes

$$\begin{aligned}\dot{\rho}_a(t)=&-\frac{|\mathfrak{p}|^2}{\hbar^2}\int_0^t\mathrm{d}\tau\sum_{\substack{\boldsymbol{k},\sigma,i,i',q,q'\\F_1,F_1',F_2,F_2'}}\mathscr{E}_k^2(\mathrm{e}^{\mathrm{i}(\omega_{F_1F_1'}-\omega_k)t-\mathrm{i}(\omega_{F_2F_2'}-\omega_k)\tau}\mathrm{e}^{\mathrm{i}\boldsymbol{k}\cdot(\boldsymbol{r}_i-\boldsymbol{r}_{i'})}D^{1*}_{q,\sigma}(\hat{\boldsymbol{k}})D^1_{q',\sigma}(\hat{\boldsymbol{k}})S^{i\dagger}_{F_1,F_1',q}S^{i'}_{F_2,F_2',q'}\rho_a(t)\\
&-\mathrm{e}^{\mathrm{i}(\omega_{F_1F_1'}-\omega_k)t-\mathrm{i}(\omega_{F_2F_2'}-\omega_k)\tau}\mathrm{e}^{\mathrm{i}\boldsymbol{k}\cdot(\boldsymbol{r}_i-\boldsymbol{r}_{i'})}D^{1*}_{q,\sigma}(\hat{\boldsymbol{k}})D^1_{q',\sigma}(\hat{\boldsymbol{k}})S^{i'}_{F_2,F_2',q'}\rho_a(t)S^{i\dagger}_{F_1,F_1',q}\\
&-\mathrm{e}^{-\mathrm{i}(\omega_{F_1F_1'}-\omega_k)t+\mathrm{i}(\omega_{F_2F_2'}-\omega_k)\tau}\mathrm{e}^{\mathrm{i}\boldsymbol{k}\cdot(\boldsymbol{r}_i-\boldsymbol{r}_{i'})}D^{1*}_{q,\sigma}(\hat{\boldsymbol{k}})D^1_{q',\sigma}(\hat{\boldsymbol{k}})S^{i'}_{F_2,F_2',q'}\rho_a(t)S^{i\dagger}_{F_1,F_1',q}\\
&+\mathrm{e}^{-\mathrm{i}(\omega_{F_1F_1'}-\omega_k)t+\mathrm{i}(\omega_{F_2F_2'}-\omega_k)\tau}\mathrm{e}^{\mathrm{i}\boldsymbol{k}\cdot(\boldsymbol{r}_i-\boldsymbol{r}_{i'})}D^{1*}_{q,\sigma}(\hat{\boldsymbol{k}})D^1_{q',\sigma}(\hat{\boldsymbol{k}})\rho_a(t)S^{i\dagger}_{F_1,F_1',q}S^{i'}_{F_2,F_2',q'}).\end{aligned} \tag{52}$$

Notice the terms $\mathrm{e}^{\pm\mathrm{i}(\omega_{F_1F_1'}-\omega_k)t\mp\mathrm{i}(\omega_{F_2F_2'}-\omega_k)\tau}$ bring difficulty to the time integral. The key point to solve this problem is to conduct a backward interaction picture transformation [12]:

$$\rho_a(t)\to\mathrm{e}^{-\mathrm{i}H_at/\hbar}\rho_a(t)\mathrm{e}^{\mathrm{i}H_at/\hbar}. \tag{53}$$

Then Eq. (52) transforms to

$$\dot{\rho}_a(t)=-\frac{\mathrm{i}}{\hbar}[H_a,\rho_a(t)] \tag{54}$$

$$\begin{aligned}&-\frac{|\mathfrak{p}|^2}{\hbar^2}\int_0^t\mathrm{d}\tau\sum_{\substack{\boldsymbol{k},\sigma,i,i',q,q'\\F_1,F_1',F_2,F_2'}}\mathscr{E}_k^2(\mathrm{e}^{\mathrm{i}(\omega_{F_2F_2'}-\omega_k)(t-\tau)}\mathrm{e}^{\mathrm{i}\boldsymbol{k}\cdot(\boldsymbol{r}_i-\boldsymbol{r}_{i'})}D^{1*}_{q,\sigma}(\hat{\boldsymbol{k}})D^1_{q',\sigma}(\hat{\boldsymbol{k}})S^{i\dagger}_{F_1,F_1',q}S^{i'}_{F_2,F_2',q'}\rho_a(t)\\
&-\mathrm{e}^{\mathrm{i}(\omega_{F_2F_2'}-\omega_k)(t-\tau)}\mathrm{e}^{\mathrm{i}\boldsymbol{k}\cdot(\boldsymbol{r}_i-\boldsymbol{r}_{i'})}D^{1*}_{q,\sigma}(\hat{\boldsymbol{k}})D^1_{q',\sigma}(\hat{\boldsymbol{k}})S^{i'}_{F_2,F_2',q'}\rho_a(t)S^{i\dagger}_{F_1,F_1',q}\\
&-\mathrm{e}^{-\mathrm{i}(\omega_{F_2F_2'}-\omega_k)(t-\tau)}\mathrm{e}^{\mathrm{i}\boldsymbol{k}\cdot(\boldsymbol{r}_i-\boldsymbol{r}_{i'})}D^{1*}_{q,\sigma}(\hat{\boldsymbol{k}})D^1_{q',\sigma}(\hat{\boldsymbol{k}})S^{i'}_{F_2,F_2',q'}\rho_a(t)S^{i\dagger}_{F_1,F_1',q}\\
&+\mathrm{e}^{-\mathrm{i}(\omega_{F_2F_2'}-\omega_k)(t-\tau)}\mathrm{e}^{\mathrm{i}\boldsymbol{k}\cdot(\boldsymbol{r}_i-\boldsymbol{r}_{i'})}D^{1*}_{q,\sigma}(\hat{\boldsymbol{k}})D^1_{q',\sigma}(\hat{\boldsymbol{k}})\rho_a(t)S^{i\dagger}_{F_1,F_1',q}S^{i'}_{F_2,F_2',q'}).\end{aligned} \tag{55}$$

Redefining S_q^i as

$$S_q^i = \sum_{F,F'} S_{F,F',q}^i, \tag{56}$$

and using the approximation $\omega_{11} \approx \omega_{12} \approx \omega_{21} \approx \omega_{22} \approx \omega_0$, we will find Eq. (55) turns to the exact same form of Eq. (29), except for an additional term $-\mathrm{i}[H_a, \rho_a(t)]/\hbar$ from backward interaction picture transformation. Thus the following deduction is the same as Sec. II.1.

II.3. Laser Coupling

Suppose there are n driving laser fields in the form of plane wave. Under dipole approximation and rotating wave approximation, the coupling Hamiltonian between laser fields and atoms is written as

$$H_l = -\sum_{i,j,q} \frac{1}{2}\hbar\Omega_j(\hat{\boldsymbol{e}}_q^* \cdot \hat{\boldsymbol{\epsilon}}_j)\mathrm{e}^{\mathrm{i}(\omega_{lj}t - \boldsymbol{k}_j\cdot\boldsymbol{r}_i)}S_q^i + \mathrm{H.c.}, \tag{57}$$

where Ω_j is the Rabi frequency of the j-th laser,

$$\Omega_j = \frac{|\mathfrak{p}|E_j}{\hbar}, \tag{58}$$

E_j, ω_{lj}, $\boldsymbol{k}_j$ and $\hat{\boldsymbol{\epsilon}}_j$ represent the magnitude, frequency, wave vector and polarization of the j-th laser beam. Here we have assumed the laser fields are at coherent states so we can treat them as classical electromagnetic waves. We put H_l into the unitary evolution term of the master equation. Incorporating with the result of Sec. II.2, we give the final form of the master equation here,

$$\begin{aligned}\dot{\rho}_a(t) = &-\frac{i}{\hbar}[H_a + H_d + H_l, \rho_a(t)] \\ &-\frac{1}{16}\Gamma\sum_{q,q'}((\beta_{q,q'}(k_0,\boldsymbol{r}) + 4\delta_{qq'})(A_{1,q}^\dagger A_{1,q'}\rho_a(t) + \rho_a(t)A_{1,q}^\dagger A_{1,q'} - 2A_{1,q'}\rho_a(t)A_{1,q}^\dagger) \\ &+(-\beta_{q,q'}(k_0,\boldsymbol{r}) + 4\delta_{qq'})(A_{2,q}^\dagger A_{2,q'}\rho_a(t) + \rho_a(t)A_{2,q}^\dagger A_{2,q'} - 2A_{2,q'}\rho_a(t)A_{2,q}^\dagger)),\end{aligned} \tag{59}$$

where H_d is the resonant dipole-dipole interaction Hamiltonian,

$$H_d = \frac{1}{16}\hbar\Gamma\sum_{q,q'}\alpha_{q,q'}(k_0,\boldsymbol{r})(A_{1,q}^\dagger A_{1,q'} - A_{2,q}^\dagger A_{2,q'}). \tag{60}$$

The definitions of α, β, A, k_0 are the same as in Sec. II.1, but the definition of S_q^i follows Eq. (56).

II.4. Quantum Trajectory Unrevealing and Recoil Effect

The master equation is a powerful tool to study atomic dynamics in laser field with position of atoms fixed. However, it can not reveal recoil effect of spontaneous emission. In addition, time evolution computation of master equation is time-consuming. Thus, a quantum trajectory unrevealing of the master equation is necessary. Quantum trajectory approach, or so called MCWF method, is proved to be equivalent to master equation approach [13]. The basic idea of MCWF method is to generate a series of quantum trajectories. These trajectories evolve according to a non-Hermitian Hamiltonian, accompanied by stochastic quantum jumps.

According to MCWF method, we should find appropriate forms of the non-Hermitian Hamiltonian and the quantum jump operators. The non-Hermitian Hamiltonian corresponding to the master equation (59) is

$$H_{eff} = H_a + H_d + H_l + H_{dec}, \tag{61}$$

where H_{dec} is the damping term,

$$H_{dec} = -\frac{\mathrm{i}\hbar\Gamma}{16}\sum_{qq'}((\beta_{q,q'}(k_0,\boldsymbol{r}) + 4\delta_{qq'})A^{\dagger}_{1,q}A_{1,q'} + (-\beta_{q,q'}(k_0,\boldsymbol{r}) + 4\delta_{qq'})A^{\dagger}_{2,q}A_{2,q'}). \tag{62}$$

The choice of quantum jump operators is not unique. It depends on what problem we are concerned. Since we are interested in the center-of-mass motion of atoms, it is important to take into account of both direction and probability of recoil for quantum jump. For single atom, the recoil effect has been discussed in [13]. The basic idea is to construct the directed-detection jump operators (or so called source-field operators). These operators are constructed according to the event of detection of photon in the far field at specific angle. Recoil arises from the momentum translation term $\exp(-\mathrm{i}\boldsymbol{k}\cdot\boldsymbol{r}_i)$ in these operators, where $\boldsymbol{r}_i$ is interpreted as atomic position operator.

In a two atom case, source-field operators can be constructed in a similar way. Carmichael [14][15] has done this work for two-level atoms. Here we extend his result to include Zeeman degeneracy. For simplicity we ignore hyperfine splitting here, but generalization to hyperfine structure is straightforward, just as what we have done in Sec. II.2. We begin with calculation of electromagnetic field generated by the atoms. In Heisenberg picture, if we consider only the interaction between atoms and the vacuum modes, the equation of motion of annihilation

operator $a_{\boldsymbol{k},\sigma}$ is

$$\begin{aligned}\dot{a}_{\boldsymbol{k},\sigma} =&\frac{\mathrm{i}}{\hbar}[H, a_{\boldsymbol{k},\sigma}]\\ =&\frac{\mathrm{i}}{\hbar}[H_a + H_{af}, a_{\boldsymbol{k},\sigma}]\\ =&-\mathrm{i}\omega_k a_{\boldsymbol{k},\sigma} - \mathrm{i}\sum_{q,i}\kappa_{\boldsymbol{k},\sigma,q,i}S_q^i,\end{aligned} \tag{63}$$

where $\kappa_{\boldsymbol{k},\sigma,q,i}$ is

$$\kappa_{\boldsymbol{k},\sigma,q,i} = -\frac{\mathfrak{p}\mathscr{E}_k}{\hbar}D^1_{q,\sigma}(\hat{\boldsymbol{k}})\mathrm{e}^{-\mathrm{i}\boldsymbol{k}\cdot\boldsymbol{r}_i}. \tag{64}$$

Define $\tilde{a}_{\boldsymbol{k},\sigma}$, $\tilde{S}_q^i$ as

$$a_{\boldsymbol{k},\sigma} =\tilde{a}_{\boldsymbol{k},\sigma}\mathrm{e}^{-\mathrm{i}\omega_k t} \tag{65}$$

$$S_q^i =\tilde{S}_q^i\mathrm{e}^{-\mathrm{i}\omega_0 t}. \tag{66}$$

The dynamics of $\tilde{a}_{\boldsymbol{k},\sigma}$ is given by

$$\dot{\tilde{a}}_{\boldsymbol{k},\sigma} = -\mathrm{i}\sum_{q,i}\kappa_{\boldsymbol{k},\sigma,q,i}\tilde{S}_q^i\mathrm{e}^{-\mathrm{i}(\omega_k-\omega_0)t}. \tag{67}$$

Integration of the above equation gives

$$\tilde{a}_{\boldsymbol{k},\sigma}(t) = \tilde{a}_{\boldsymbol{k},\sigma}(0) - \mathrm{i}\sum_{q,i}\kappa_{\boldsymbol{k},\sigma,q,i}\int_0^t \mathrm{d}t'\ \tilde{S}_q^i(t')\mathrm{e}^{\mathrm{i}(\omega_k-\omega_0)t'}. \tag{68}$$

Suppose the field is initially at vacuum state. We see the first term of Eq. (68) corresponds to vacuum electromagnetic field. The second term of Eq. (68) corresponds to the field radiated by the atoms, which is

$$\boldsymbol{E}_s^{(+)}(\boldsymbol{R},t) = -\mathrm{i}\sum_{\boldsymbol{k},\sigma,q,i}\kappa_{\boldsymbol{k},\sigma,q,i}\mathscr{E}_k\hat{\boldsymbol{\epsilon}}^*_{\boldsymbol{k},\sigma}\mathrm{e}^{\mathrm{i}(\boldsymbol{k}\cdot\boldsymbol{R}-\omega_0 t)}\int_0^t \mathrm{d}t'\ \tilde{S}_q^i(t')\mathrm{e}^{\mathrm{i}(\omega_k-\omega_0)(t'-t)}. \tag{69}$$

Choosing helicity polarization vectors and rearranging Eq. (69), we have

$$\begin{aligned}\boldsymbol{E}_s^{(+)}(\boldsymbol{R},t) =&\mathrm{i}\sum_{\boldsymbol{k},\sigma,q,q',i}\frac{\mathfrak{p}\omega_k}{2\epsilon_0 V}D^1_{q,\sigma}(\hat{\boldsymbol{k}})D^{1*}_{q',\sigma}(\hat{\boldsymbol{k}})\hat{\boldsymbol{e}}^*_{q'}\mathrm{e}^{\mathrm{i}(\boldsymbol{k}\cdot(\boldsymbol{R}-\boldsymbol{r}_i)-\omega_0 t)}\int_0^t \mathrm{d}t'\ \tilde{S}_q^i(t')\mathrm{e}^{\mathrm{i}(\omega_k-\omega_0)(t'-t)}\\ =&\mathrm{i}\sum_{\boldsymbol{k},q,q',i}\frac{\mathfrak{p}\omega_k}{2\epsilon_0 V}\hat{\boldsymbol{e}}^*_{q'}\mathrm{e}^{\mathrm{i}(\boldsymbol{k}\cdot(\boldsymbol{R}-\boldsymbol{r}_i)-\omega_0 t)}(\delta_{qq'} - D^1_{q,0}(\hat{\boldsymbol{k}})D^{1*}_{q',0}(\hat{\boldsymbol{k}}))\int_0^t \mathrm{d}t'\ \tilde{S}_q^i(t')\mathrm{e}^{\mathrm{i}(\omega_k-\omega_0)(t'-t)}\\ =&\frac{\mathrm{i}\mathfrak{p}}{16\pi^3c^3\epsilon_0}\sum_{q,q',i}\int_0^\infty \mathrm{d}\omega_k\ \omega_k^3\int \mathrm{d}\Omega_k\hat{\boldsymbol{e}}^*_{q'}\mathrm{e}^{\mathrm{i}(\boldsymbol{k}\cdot\boldsymbol{R}_i-\omega_0 t)}(\delta_{qq'} - D^1_{q,0}(\hat{\boldsymbol{k}})D^{1*}_{q',0}(\hat{\boldsymbol{k}}))\\ &\times\int_0^t \mathrm{d}t'\ \tilde{S}_q^i(t')\mathrm{e}^{\mathrm{i}(\omega_k-\omega_0)(t'-t)},\end{aligned} \tag{70}$$

where we have replaced $(\boldsymbol{R}-\boldsymbol{r}_i)$ with $\boldsymbol{R}_i$. The integral over unit sphere in k-space is similar to the integral we have dealt with in App. A. We give the result here,

$$\int \mathrm{d}\Omega_k \hat{\boldsymbol{e}}^*_{q'} \mathrm{e}^{\mathrm{i}\boldsymbol{k}\cdot\boldsymbol{R}_i}(\delta_{qq'} - D^1_{q,0}(\hat{\boldsymbol{k}})D^{1*}_{q',0}(\hat{\boldsymbol{k}})) = \frac{2\pi}{3}\beta^{\mathrm{T}}_{q,q'}(k,\boldsymbol{R}_i), \tag{71}$$

Where $\beta_{q,q'}$ is defined in Eq. (44). For the reason that only far field is concerned, we take the limit $R_i \to \infty$ and ignore the terms higher than R_i^{-1} in Eq. (71), we have

$$\beta(k,\boldsymbol{R}_i) \to j_0(kR_i)\gamma(\hat{\boldsymbol{R}}_i) = \frac{\sin(kR_i)}{kR_i}\gamma(\hat{\boldsymbol{R}}_i), \tag{72}$$

where

$$\gamma(\hat{\boldsymbol{R}}_i) = \begin{pmatrix} 4+2P_2(\cos\theta_{R_i}) & \sqrt{2}\mathrm{e}^{-\mathrm{i}\phi_{R_i}}P_2^1(\cos\theta_{R_i}) & \mathrm{e}^{-2\mathrm{i}\phi_{R_i}}P_2^2(\cos\theta_{R_i}) \\ \sqrt{2}\mathrm{e}^{-\mathrm{i}\phi_{R_i}}P_2^1(\cos\theta_{R_i}) & 4-4P_2(\cos\theta_{R_i}) & -\sqrt{2}\mathrm{e}^{-\mathrm{i}\phi_{R_i}}P_2^1(\cos\theta_{R_i}) \\ \mathrm{e}^{-2\mathrm{i}\phi_{R_i}}P_2^2(\cos\theta_{R_i}) & -\sqrt{2}\mathrm{e}^{-\mathrm{i}\phi_{R_i}}P_2^1(\cos\theta_{R_i}) & 4+2P_2(\cos\theta_{R_i}) \end{pmatrix}. \tag{73}$$

Eq. (70) becomes

$$\boldsymbol{E}^{(+)}_s(\boldsymbol{R},t) = \sum_{q,q',i} \frac{\mathrm{i}\mathfrak{p}\gamma^{\mathrm{T}}_{q,q'}(\hat{\boldsymbol{R}}_i)\hat{\boldsymbol{e}}^*_{q'}}{24\pi^2c^2\epsilon_0 R_i}\int_0^\infty \mathrm{d}\omega_k\ \omega_k^2 \sin(\frac{\omega_k}{c}R_i)\mathrm{e}^{-\mathrm{i}\omega_0 t}\int_0^t \mathrm{d}t'\ \tilde{S}^i_q(t')\mathrm{e}^{\mathrm{i}(\omega_k-\omega_0)(t'-t)}. \tag{74}$$

Now we focus on the integrals in Eq. (74), i.e.,

$$\int_0^\infty \mathrm{d}\omega_k\ \omega_k^2 \sin(\frac{\omega_k}{c}R_i)\mathrm{e}^{-\mathrm{i}\omega_0 t}\int_0^t \mathrm{d}t'\ \tilde{S}^i_q(t')\mathrm{e}^{\mathrm{i}(\omega_k-\omega_0)(t'-t)}. \tag{75}$$

Under Markovian approximation, the system has no memory. Accordingly, the electromagnetic field at time t and position $\boldsymbol{R}$ only depends on the state of atom at time $(t - R_i/c)$, where R_i/c comes from the retardation effect. Therefore we replace $\tilde{S}^i_q(t')$ in Eq. (75) with $\tilde{S}^i_q(t - R_i/c)$,

$$\begin{aligned}
&\int_0^\infty \mathrm{d}\omega_k\ \omega_k^2 \sin(\frac{\omega_k}{c}R_i)\mathrm{e}^{-\mathrm{i}\omega_0 t}\int_0^t \mathrm{d}t'\ \tilde{S}^i_q(t')\mathrm{e}^{\mathrm{i}(\omega_k-\omega_0)(t'-t)} \\
\approx&\int_0^\infty \mathrm{d}\omega_k\ \omega_k^2 \sin(\frac{\omega_k}{c}R_i)\mathrm{e}^{-\mathrm{i}\omega_0 t}\tilde{S}^i_q(t-\frac{R_i}{c})\int_0^t \mathrm{d}t'\ \mathrm{e}^{\mathrm{i}(\omega_k-\omega_0)(t'-t)} \\
\approx&\int_0^\infty \mathrm{d}\omega_k\ \omega_k^2 \sin(\frac{\omega_k}{c}R_i)\mathrm{e}^{-\mathrm{i}\omega_0 t}\tilde{S}^i_q(t-\frac{R_i}{c})(\pi\delta(\omega_0-\omega_k)+\mathrm{i}P(\frac{1}{\omega_0-\omega_k})) \\
=&\mathrm{e}^{-\mathrm{i}\omega_0 t}\tilde{S}^i_q(t-\frac{R_i}{c})\int_0^\infty \mathrm{d}\omega_k\ \omega_k^2 \sin(\frac{\omega_k}{c}R_i)(\pi\delta(\omega_0-\omega_k)+\mathrm{i}P(\frac{1}{\omega_0-\omega_k})) \\
\approx&\mathrm{e}^{-\mathrm{i}\omega_0 t}\tilde{S}^i_q(t-\frac{R_i}{c})\pi\omega_0^2(\sin(k_0R_i)-\mathrm{i}\cos(k_0R_i)),
\end{aligned} \tag{76}$$

Where we have applied the results of Eq. (40) and App. B. Then Eq. (74) becomes

$$\begin{aligned}\boldsymbol{E}_s^{(+)}(\boldsymbol{R},t) =& \sum_{q,q',i} \frac{\mathfrak{p}\omega_0^2 \gamma^{\mathrm{T}}_{q,q'}(\hat{\boldsymbol{R}}_i)\hat{\boldsymbol{e}}^*_{q'}}{24\pi c^2\epsilon_0 R_i} \tilde{S}^i_q(t-\frac{R_i}{c})\mathrm{e}^{\mathrm{i}(k_0R_i-\omega_0 t)} \\ =& \sum_{q,q',i} \frac{\mathfrak{p}\omega_0^2 \gamma^{\mathrm{T}}_{q,q'}(\hat{\boldsymbol{R}}_i)\hat{\boldsymbol{e}}^*_{q'}}{24\pi c^2\epsilon_0 R_i} S^i_q(t-\frac{R_i}{c}) \\ =& \sum_{q'} \hat{\boldsymbol{e}}^*_{q'} E^{(+)}_{s,q'}(\boldsymbol{R},t),\end{aligned} \tag{77}$$

where

$$E^{(+)}_{s,q'}(\boldsymbol{R},t) = \sum_{q,i} \frac{\mathfrak{p}\omega_0^2 \gamma^{\mathrm{T}}_{q,q'}(\hat{\boldsymbol{R}}_i)}{24\pi c^2\epsilon_0 R_i} S^i_q(t-\frac{R_i}{c}) \tag{78}$$

is the q' component of electromagnetic field in spherical basis. Following the approximation in [16] and assuming $|\boldsymbol{r}_1-\boldsymbol{r}_2| \ll R$, we have

$$\begin{aligned}E^{(+)}_{s,q'}(\boldsymbol{R},\frac{R}{c}) \approx& \sum_{q,i} \frac{\mathfrak{p}\omega_0^2 \gamma^{\mathrm{T}}_{q,q'}(\hat{\boldsymbol{R}})}{24\pi c^2\epsilon_0 R} S^i_q(0)\mathrm{e}^{\mathrm{i}k_0(R_i-r)} \\ \approx& \sum_{q,i} \frac{\mathfrak{p}\omega_0^2 \gamma^{\mathrm{T}}_{q,q'}(\hat{\boldsymbol{R}})}{24\pi c^2\epsilon_0 R} S^i_q(0)\mathrm{e}^{-\mathrm{i}k_0\hat{\boldsymbol{R}}\cdot\boldsymbol{r}_i}.\end{aligned} \tag{79}$$

According to [14], we define the scaled source-field operators

$$\begin{aligned}O_{q'}(\hat{\boldsymbol{R}}) =& \sqrt{\frac{2\epsilon_0 c}{\hbar\omega_0} R^2 \sin\theta_R \mathrm{d}\theta_R \mathrm{d}\phi_R} E^{(+)}_{s,q'}(\boldsymbol{R},\frac{R}{c}) \\ =& \sqrt{\frac{2\epsilon_0 c}{\hbar\omega_0} \sin\theta_R \mathrm{d}\theta_R \mathrm{d}\phi_R} \sum_{q,i} \frac{\mathfrak{p}\omega_0^2 \gamma^{\mathrm{T}}_{q,q'}(\hat{\boldsymbol{R}})}{24\pi c^2\epsilon_0} S^i_q \mathrm{e}^{-\mathrm{i}k_0\hat{\boldsymbol{R}}\cdot\boldsymbol{r}_i},\end{aligned} \tag{80}$$

where we have replace $S^i_q(0)$ with Schrödinger operator S^i_q. The source-field operators satisfy the super-operator identity

$$\begin{aligned}\sum_q \int O_q(\hat{\boldsymbol{R}}) \cdot O^\dagger_q(\hat{\boldsymbol{R}}) = \frac{1}{8}\Gamma \sum_{q,q'} &((\beta_{q,q'}(k_0,\boldsymbol{r})+4\delta_{qq'})(A_{1,q'}\cdot A^\dagger_{1,q}) \\ &+(-\beta_{q,q'}(k_0,\boldsymbol{r})+4\delta_{qq'})(A_{2,q'}\cdot A^\dagger_{2,q})),\end{aligned} \tag{81}$$

which confirms that $O_q(\hat{\boldsymbol{R}})$ is a set of jump operators to unravel the master equation (59). Notice

$$\langle\psi(t)| O^\dagger_q(\hat{\boldsymbol{R}}) O_q(\hat{\boldsymbol{R}}) |\psi(t)\rangle \,\mathrm{d}t \tag{82}$$

is the photon detection probability at the solid angel $(\sin\theta_R \mathrm{d}\theta_R \mathrm{d}\phi_R)$ in the time interval $t \to t + \mathrm{d}t$ with photon polarization q. Thus, $O_q(\hat{\boldsymbol{R}})$ can be interpreted as the back action of photon detection upon the atomic wave function. Specifically, if we detect a photon in the time interval $t \to t + \mathrm{d}t$ with photon polarization q at the solid angel $(\sin\theta_R \mathrm{d}\theta_R \mathrm{d}\phi_R)$, the back action of this observation upon the atoms is $O_q(\hat{\boldsymbol{R}}) |\psi(t)\rangle$. Notice the term $\mathrm{e}^{-\mathrm{i}k_0 \hat{\boldsymbol{R}}\cdot\boldsymbol{r}_i}$ in Eq. (80). If we reinterpret the wave function $|\psi(t)\rangle$ as a tensor product of the center-of-mass motion wave function and the internal state wave function, the action of the term $\mathrm{e}^{-\mathrm{i}k_0 \hat{\boldsymbol{R}}\cdot\boldsymbol{r}_i}$ is actually recoil effect. However, $O_q(\hat{\boldsymbol{R}})$ is a sum over operators acting on two atoms. The action of $O_q(\hat{\boldsymbol{R}})$ on $|\psi(t)\rangle$ will generate entanglement between internal and external states, which brings difficulty to our semi-classical simulation. We argue that the entanglement decoherent rapidly compared to the atomic collision time interval ($\sim 1\ \mu$s) due to the randomness of atomic motion. We will handle quantum jump in simulation in this way: if a quantum jump happens, act the corresponding jump operator $O_q(\hat{\boldsymbol{R}})$ on the internal state wave function and choose one of the atoms randomly to give it momentum $-k_0\hat{\boldsymbol{R}}$.

II.5. Force Operator

As mentioned in Sec. I, we will treat the center-of-mass motion of atoms classically. Thus, we use the Heisenberg-picture force operator

$$\boldsymbol{F}_i = \dot{\boldsymbol{p}}_i = \frac{\mathrm{i}}{\hbar}[H, \boldsymbol{p}_i] = -\nabla_{\boldsymbol{r}_i} H \tag{83}$$

to calculate the force exerted on the i-th atom,

$$\boldsymbol{f}_i(t) = \langle F_i \rangle = -\langle \psi(t)| \nabla_{\boldsymbol{r}_i} H |\psi(t)\rangle . \tag{84}$$

Because

$$H = H_a + H_d + H_l, \tag{85}$$

we have included both dipole-dipole force and light force in Eq. (84).

III. SIMULATION

III.1. D1 Molasses

In consideration of our experimental setup, we hope to achieve 3D complete optical shielding in ^{39}K D1 molasses. Our simulation is based on this motivation.

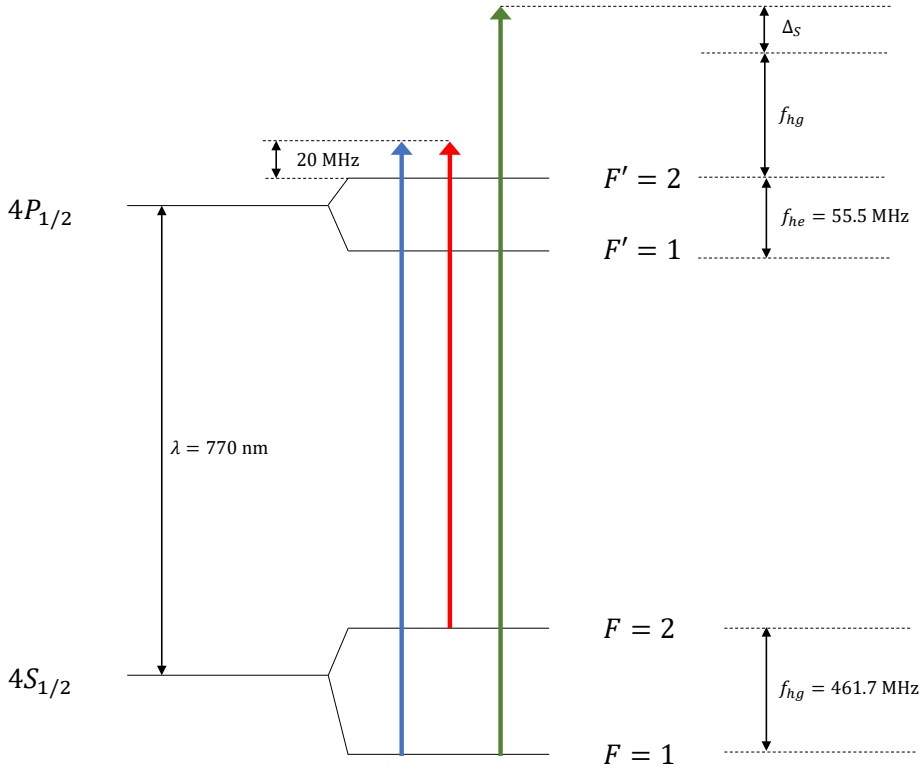

FIG. 4: ^{39}K D1 molasses scheme and the shielding laser. The cooling laser (in blue) is blue detuned from the transition $|F = 1\rangle \rightarrow |F' = 2\rangle$ by 20MHz, and the repumping laser (in red) is blue detuned from the transition $|F = 2\rangle \rightarrow |F' = 2\rangle$ by 20MHz. The shielding laser (in green) is blue detuned from the transition $|F = 1\rangle \rightarrow |F' = 2\rangle$ by $\omega_{hg} + \Delta_S$.

A typical ^{39}K D1 molasses scheme is shown in Fig. 4. Two sidebands of D1 lasers have frequency difference equal to ω_{hg} and are both blue detuned by 20MHz. The D1 molasses lasers are shone from six directions $(\pm x, \pm y, \pm z)$. Each beam is circular polarized. Counter-propagating beams have opposite polarizations. The saturation parameters of cooling and repumping lasers are set to 10 and 2. Our plan is to add blue detuned shielding beams in addition to the D1 molasses beams to shield atoms.

III.2. Dressed Ground States Potential

Before we start to do dynamical simulation, we need some indications about how to select parameters for the shielding beams. Therefore, we calculate the energy spectrum of the dressed two atom ground states in monochromatic laser fields. This calculation will show us the effects of shielding beams or D1 molasses beams on ground state molecular potential between atoms.

Since laser fields are monochromatic, a rotating wave transformation can remove the time-dependence of the Hermitian part of the Hamiltonian $H = H_a + H_d + H_l$. H has the dependence of atomic position $\boldsymbol{r}_1, \boldsymbol{r}_2$. We calculate the eigenvalues of H at different atomic position, and the projection of each eigenstates on ground states. Then we pick out 64 eigenstates with the largest projection on ground states and plot the eigenvalues of these states versus atomic distance r (64 because ^{39}K has 8 ground).

We first plot the energy spectrum in the effect of the repumping lasers. We find the repumping lasers couple the ground state $|F = 1\rangle_1 \otimes |F = 1\rangle_2$ with the attractive molecular potential. Consequently, the coupling opens an attractive gap at $r = 0.026$ μm, as shown in Fig. 5.

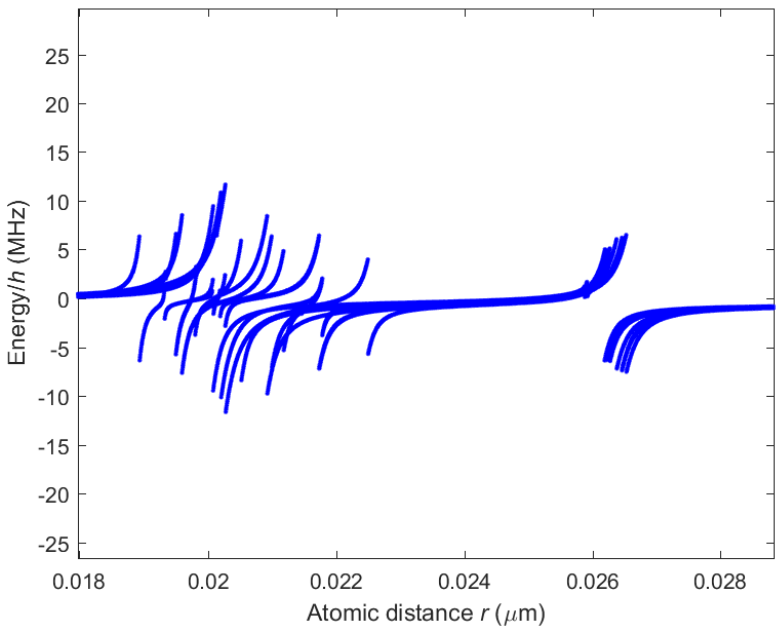

FIG. 5: Energy spectrum of $|F = 1, M\rangle_1 \otimes |F = 1, M\rangle_2$ with repumping lasers dressing. Atoms are displaced in y direction.

To compensate the effect of these repulsive potential generated by the repumping lasers, we properly tune the frequency of shielding laser to open a repulsive gap for the dressed $|F=1,M\rangle_1 \otimes |F=1,M\rangle_2$ state at $r > 0.026\mu$m. We find it is appropriate to blue detune the shielding laser to the $|F=1\rangle \rightarrow |F'=2\rangle$ transition by $\omega_{hg} + \Delta_S$, as shown in Fig. 4. In this frequency, the shielding laser will not interfere the D1 cooling process since its detuning is larger than about 500 MHz. In addition, it will couple the $|F=1,M\rangle_1 \otimes |F=1,M\rangle_2$ state with the repulsive molecular state corresponding to $|F=2,M\rangle \otimes |F'=2,M\rangle$. Besides, we find that circular polarization opens larger gap than linear polarization. So we adopt circular polarization for shielding lasers. Based on classical intuition, we set the directions of shielding beams as $(+x,+y)$ in order to achieve 3D shielding effect. As shown in Fig 6, the shielding lasers open a gap at $r = 0.032\mu$m for both atomic configurations, for which we postulate that this shielding laser configuration can shield atoms from attracting each other in different directions.

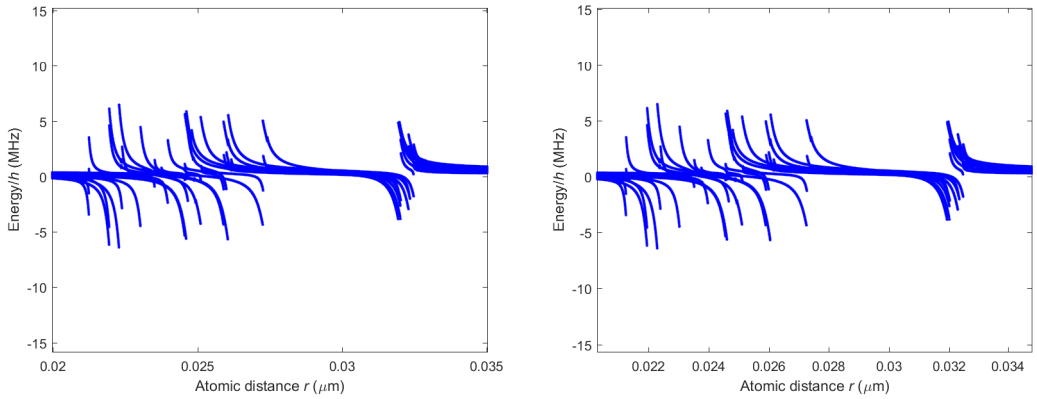

FIG. 6: Energy spectrum of $|F=1,M\rangle_1 \otimes |F=1,M\rangle_2$ with shileding lasers dressing. Left: atoms are displaced in y direction. Right: atoms are displaced in z direction. Detuning is chosen as $\Delta_S = 0.5\omega_{hg}$. Saturation parameter is 35 for each beam.

III.3. Aspects of The Simulation Method

To testify our postulation in Sec. III.2, we carry out dynamical simulation. Based on MCWF method, a statistical way of study is applied, i.e., we repeatedly simulate the dynamics of atoms for many trials in certain conditions and compare statistical results of simulation in different conditions. Bellow are our simulation steps.

Firstly we set up initial condition. The initial wave function $|\psi\rangle_i$ is set as a tensor product of two randomly chosen ground states. The relative direction of atoms and initial positions are set randomly with the initial atomic distance r_0 fixed for the convenience of comparison. The center-of-mass velocity of two atoms is set to be zero. The magnitude of initial relative velocity v_0 is fixed. The two atoms are set to move towards each other initially. Besides, we discretize the space into about 100 solid angles in order to calculate the source-field jump operators $O_q(\hat{\boldsymbol{R}})$.

During simulation, the wave function $|\psi(t)\rangle$ evolves with H_{eff} when no quantum jump happens. The nuclear motion of atoms are subjected to the force $\boldsymbol{f}_i(t)$ under Newton's laws. During each time step, a random number between 0 and 1 is generated and the norm of $|\psi(t)\rangle$ is compared to this number. If the norm is larger than the number then a quantum jump is carried out in this step, otherwise no jump happens in the step. In any case $|\psi(t)\rangle$ is renormalized in the end of each time step. If a quantum jump happens, the expectation value $\langle\psi(t)|\, O_q^\dagger(\hat{\boldsymbol{R}})O_q(\hat{\boldsymbol{R}})\,|\psi(t)\rangle$ is calculated for each solid angle. One angle is chosen weighted-randomly according to the expectation values. Then we act the corresponding jump operator $O_q(\hat{\boldsymbol{R}})$ on $|\psi(t)\rangle$ and randomly chose one atom to give it the back action momentum $-k_0\hat{\boldsymbol{R}}$.

If the atomic distance is below a criterion r_c or the atomic velocity is larger than a criterion v_c, the simulation will cease and this trial will be marked as failed. Otherwise, if the atomic distance returns back to r_0, the simulation will stop and this trial will be marked as succeed.

The simulation parameters are listed bellow in Tab. I. Notice that we choose time step $\mathrm{d}t$ according to the largest frequency in the Hamiltonian, i.e., $2\omega_{hg}$.

III.4. Results

We scan both frequency and intensity of the shielding lasers. For each condition, 100 trails are carried out. The success rate (the probability atoms repulse each other) is a

TABLE I: Simulation parameters

$r_0/\mu\mathrm{m}$	$v_0/\mathrm{m}\cdot\mathrm{s}^{-1}$	$r_c/\mu\mathrm{m}$	$v_c/\mathrm{m}\cdot\mathrm{s}^{-1}$	$\mathrm{d}t/\mu\mathrm{s}$
0.1	0.1	2.33	0.01	5.4×10^{-5}

proper measure of shielding effect. We compare the success rates in different conditions, as shown in Fig 7, 8.

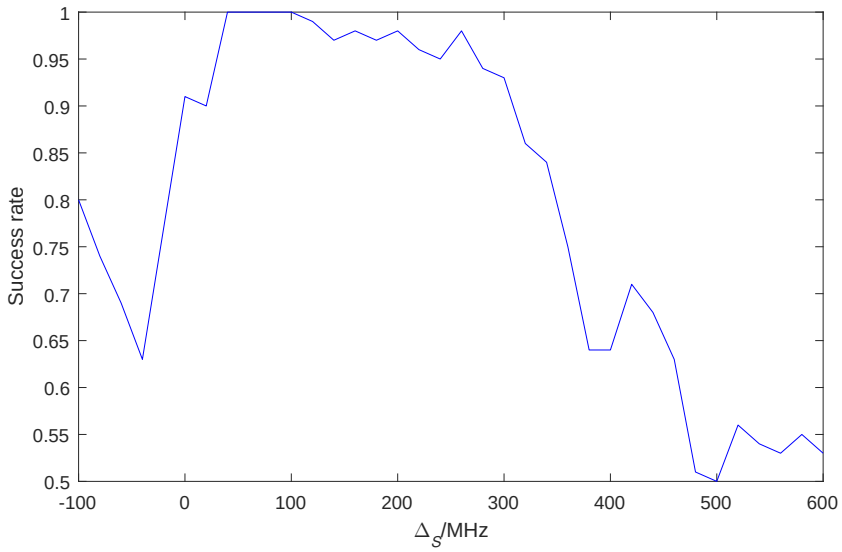

FIG. 7: Success rate in different Δ_S. Saturation parameter is fixed to 35

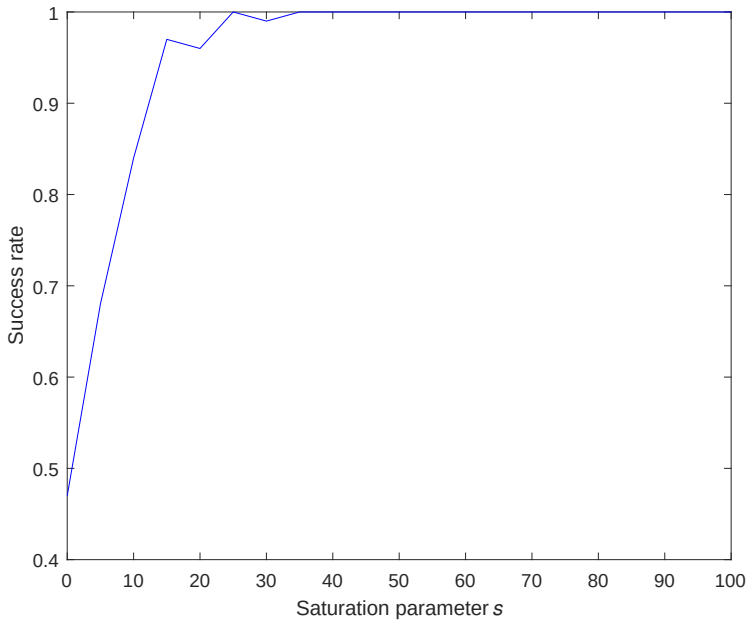

FIG. 8: Success rate in different s. Δ_S is fixed to $0.1\omega_{hg}$

Notice in Fig 7, the success rate has a dip when $\Delta_S < 0$, which is reasonable since red detuning laser couples the ground state to attractive potential. The shielding effect reaches

optimum at $\Delta_S = 100$ MHz and decreases as frequency increases. In Fig. 8, we find the shielding effect stays good when $s > 40$.

IV. EXPERIMENTAL VERIFICATION

Ultimately, we will test our theory experimentally in degenerate atomic gas and conduct non-demolishing detection of two atoms. Before that, a test of the theory in dipole trap is necessary and easier to conduct. Cold atoms in dipole trap will escape from the trap due to cold collision, and population of atoms in dipole trap will decay exponentially. A typical way to measure the shielding effect is to measure the rate of population decay [2], because optical shielding can avoid cold collision and diminish the rate of decay. We plan to conduct such an experiment. Specifically, we will shine shielding lasers on a ^{39}K D1 molasses in dipole trap. We will measure the rate of decay with different laser parameters and different laser configurations. The population of atom sample will be measured by absorption image or fluorescence.

V. DISCUSSION AND CONCLUSIONS

Appendix A: Integral Over Unit Sphere in k-space

In this appendix we give the deduction for Eq. (39). Firstly we focus on $I^{11}_{q,q'}(k)$, i.e.

$$\begin{aligned} I^{11}_{q,q'}(k) &= \sum_{\sigma=\pm1} \int \mathrm{d}\Omega_k \; X^*_{1,q,\sigma,\boldsymbol{k}} X_{1,q',\sigma,\boldsymbol{k}} \\ &= \sum_{\sigma=\pm1} \int \mathrm{d}\Omega_k \; D^{1*}_{q,\sigma}(\hat{\boldsymbol{k}}) D^{1}_{q',\sigma}(\hat{\boldsymbol{k}}) \cos^2(\boldsymbol{k}\cdot\boldsymbol{r}/2). \end{aligned} \tag{A1}$$

Expressing the Wigner D-matrix $D^1_{q,\sigma}(\hat{\boldsymbol{k}})$ in Euler angles form and applying the orthogonality of $D^1_{q,\sigma}(\hat{\boldsymbol{k}})$, we have

$$\begin{aligned} \sum_{\sigma=\pm1} D^{1*}_{q,\sigma}(\hat{\boldsymbol{k}}) D^{1}_{q',\sigma}(\hat{\boldsymbol{k}}) &= \sum_{\sigma=\pm1} D^{1*}_{q,\sigma}(\phi_k,\theta_k,0) D^{1}_{q',\sigma}(\phi_k,\theta_k,0) \\ &= \delta_{q,q'} - D^{1*}_{q,0}(\phi_k,\theta_k,0) D^{1}_{q',0}(\phi_k,\theta_k,0), \end{aligned} \tag{A2}$$

where ϕ_k, θ_k are azimuthal and polar angles in $\boldsymbol{k}$-space. According to plane wave expansion,

$$\cos^2(\boldsymbol{k}\cdot\boldsymbol{r}/2) = \frac{1}{2}(1+\cos(\boldsymbol{k}\cdot\boldsymbol{r})) = \frac{1}{2} + 2\pi\mathrm{Re}(\sum_{l=0}^{\infty}\sum_{m=-l}^{m=l} \mathrm{i}^l j_l(kr) Y_l^{m*}(\theta_k,\phi_k) Y_l^m(\theta_r,\phi_r)), \tag{A3}$$

where Re means taking the real part. According to the relation between Wigner D-matrix and spherical harmonics $Y_l^m(\theta,\phi)$:

$$Y_l^m(\theta,\phi) = \sqrt{\frac{2l+1}{4\pi}} D^{l*}_{m,0}(\phi,\theta,0), \tag{A4}$$

we rewrite Eq. (A1) as

$$\begin{aligned} I^{11}_{q,q'}(k) = \frac{1}{2}\int \mathrm{d}\Omega_k \ (\delta_{q,q'} - \frac{4\pi}{3} Y_1^q(\theta_k,\phi_k) Y_1^{q*}(\theta_k,\phi_k)) \\ \times (1 + 4\pi\mathrm{Re}(\sum_{l=0}^{\infty}\sum_{m=-l}^{m=l} \mathrm{i}^l j_l(kr) Y_l^{m*}(\theta_k,\phi_k) Y_l^m(\theta_r,\phi_r))). \end{aligned} \tag{A5}$$

The integral over the unit sphere in $\boldsymbol{k}$-space can be done by applying the formula

$$\int \mathrm{d}\Omega \ Y_{l_3}^{m_3 *} Y_{l_1}^{m_1} Y_{l_2}^{m_2} = \sqrt{\frac{(2l_1+1)(2l_2+1)}{4\pi(2l_3+1)}} \langle l_3, m_3 | l_1, l_2, m_1, m_2\rangle \langle l_1, l_2, 0, 0 | l_3, 0\rangle, \tag{A6}$$

which indicates only the terms with $l = 0$ or 2 survive in the summation of Eq. A5. The final result is given in Eq. 41.

The deduction for $I^{22}_{q,q'}$ is similar. The only difference is a change of sign. $I^{12}_{q,q'}$ and $I^{21}_{q,q'}$ give zeros because

$$\sin(\boldsymbol{k}\cdot\boldsymbol{r}/2)\cos(\boldsymbol{k}\cdot\boldsymbol{r}/2) = \frac{1}{2}\sin(\boldsymbol{k}\cdot\boldsymbol{r}) = 2\pi\mathrm{Im}(\sum_{l=0}^{\infty}\sum_{m=-l}^{m=l} \mathrm{i}^l j_l(kr) Y_l^{m*}(\theta_k,\phi_k) Y_l^m(\theta_r,\phi_r)), \tag{A7}$$

and taking imaginary part gives odd l.

Appendix B: k-Integral

The integrals we need to calculate takes the form

$$\int_0^{\infty} \mathrm{d}\omega_k \ (\frac{\omega_k}{\omega_0})^3 P(\frac{1}{\omega_0 - \omega_k}) j_l(\frac{\omega_k}{c} r). \tag{B1}$$

According to [17], if we change the lower limit in the integral to $-\infty$ and use counter integration, we have

$$\int_{-\infty}^{\infty} \mathrm{d}\omega_k \ (\frac{\omega_k}{\omega_0})^3 P(\frac{1}{\omega_0 - \omega_k}) j_0(\frac{\omega_k}{c} r) = \pi n_0(k_0 r) \tag{B2}$$

$$\int_{-\infty}^{\infty} \mathrm{d}\omega_k \ (\frac{\omega_k}{\omega_0})^3 P(\frac{1}{\omega_0 - \omega_k}) j_2(\frac{\omega_k}{c} r) = \pi n_2(k_0 r), \tag{B3}$$

which gives the result in Eq. 47.

---

* xchai13@fudan.edu.cn

[1] M. Holland, K.-A. Suominen, and K. Burnett, Physical review letters **72**, 2367 (1994).

[2] J. Weiner, V. S. Bagnato, S. Zilio, and P. S. Julienne, Reviews of Modern Physics **71**, 1 (1999).

[3] M. Germann, T. Latychevskaia, C. Escher, and H.-W. Fink, Physical review letters **104**, 095501 (2010).

[4] K.-A. Suominen, M. J. Holland, K. Burnett, and P. Julienne, Physical Review A **51**, 1446 (1995).

[5] R. Napolitano, J. Weiner, and P. S. Julienne, Physical Review A **55**, 1191 (1997).

[6] V. Yurovsky and A. Ben-Reuven, Physical Review A **55**, 3772 (1997).

[7] S. Muniz, L. Marcassa, R. Napolitano, G. Telles, J. Weiner, S. Zilio, and V. Bagnato, Physical Review A **55**, 4407 (1997).

[8] J. Piilo and K.-A. Suominen, Physical Review A **66**, 013401 (2002).

[9] F. Sievers, N. Kretzschmar, D. R. Fernandes, D. Suchet, M. Rabinovic, S. Wu, C. V. Parker, L. Khaykovich, C. Salomon, and F. Chevy, Physical Review A **91**, 023426 (2015).

[10] G. Lenz and P. Meystre, Physical Review A **48**, 3365 (1993).

[11] E. Goldstein, P. Pax, and P. Meystre, Physical Review A **53**, 2604 (1996).

[12] R. R. Puri, *Mathematical methods of quantum optics*, Vol. 79 (Springer Science & Business Media, 2001).

[13] K. Mølmer, Y. Castin, and J. Dalibard, JOSA B **10**, 524 (1993).

[14] H. Carmichael and K. Kim, Optics communications **179**, 417 (2000).

[15] H. Carmichael, *An open systems approach to quantum optics: lectures presented at the Université Libre de Bruxelles, October 28 to November 4, 1991*, Vol. 18 (Springer Science & Business

Media, 2009).

[16] R. Lehmberg, Physical Review A **2**, 883 (1970).

[17] J. Piilo, K.-A. Suominen, and K. Berg-Soørensen, Physical Review A **65**, 033411 (2002).